# Brain Tumors

# 11

Giampiero Giovacchini, Victoria Salati, and Valentina Garibotto

## 11.1 Introduction

Primary brain tumors are a heterogeneous group of neoplasms, each with its own biology, prognosis, and treatment. Among primary brain tumors, gliomas constitute the most frequent pathologic finding. On the basis of histological features, gliomas are dived into low-grade (I and II) and high-grade (III and IV) tumors. Prognosis worsens as tumor grading increases. Brain tumors may remain asymptomatic for long periods. The most common symptom is headache. Focal symptoms or signs take place when the neoplasm compresses the nearby cerebral parenchyma.

In this chapter we will review the main features of neoplasms of the central nervous system (CNS), and we will focus on the use of positron emission tomography (PET) and single photon emission computed tomography (SPECT) and of hybrid techniques, particularly PET with computed tomography (PET/CT) and PET with magnetic resonance (PET/MR) in combination with various radiopharmaceuticals for the diagnosis, treatment, and follow-up of gliomas (Table 11.1).

G. Giovacchini (✉)
Institute of Radiology and Nuclear Medicine, Stadtspital Triemli, Zurich, Switzerland
e-mail: giovacchinig@yahoo.com

V. Salati • V. Garibotto
Department of Medical Imaging, Geneva University and Geneva University Hospitals, Geneva, Switzerland

## 11.2 Brain Tumor Imaging

### 11.2.1 Radiolabeled Amino Acids

The rate of protein synthesis is increased in proliferating brain tumors, which makes its measurement an important target for in vivo imaging. Uptake in the normal cortex of all labeled amino acids is very low and their role in mediating an inflammatory response is much less important than for glucose. Thus, high specificity could be predicted. Active transport through the natural amino acid carrier and, to some extent, blood–brain barrier (BBB) disruption represent the mechanisms of tracer uptake (Table 11.2).

**$^{11}$C-Methionine** Methionine, an essential sulfur amino acid, is necessary for growth and development. $^{11}$C-Methionine ($^{11}$C-MET) is by far the amino acid most frequently used for brain tumor imaging.

*Diagnostic Accuracy* The overall sensitivity of $^{11}$C-MET PET for distinguishing gliomas from nonmalignant lesions has been estimated to be around 75–95 %, with somewhat lower values reported in low-grade gliomas, where uptake


A. Ciarmiello, L. Mansi (eds.), *PET-CT and PET-MRI in Neurology*,
DOI 10.1007/978-3-319-31614-7_11

**Table 11.1** Clinical indications to imaging gliomas

| |
|---|
| Pre-therapy |
| 1. Diagnosis |
| 2. Noninvasive tumor grading |
| 3. Guidance for stereotactic biopsy |
| 4. Surgical planning |
| 5. Identification of metabolically active tumor (or biological target volume, BTV) for radiotherapy planning |
| Post-therapy |
| 1. Identification of residual tumor |
| 2. Differential diagnosis between tumor recurrence and radiation necrosis |
| 3. Evaluation of response to chemotherapy |
| 4. Prediction of survival |

**Table 11.2** Most common current radiotracers for brain tumor imaging

| Biological process | Radiotracer |
|---|---|
| Glucose transport across BBB and metabolism | [$^{18}$F]-Fluodeoxyglucose ([$^{18}$F]-FDG) |
| Amino acid transport and protein synthesis | [$^{11}$C]-Leucine<br>$^{11}$C-Methionine ($^{11}$C-MET)<br>[$^{123}$I]-Alpha-methyltyrosine ([$^{123}$I]-IMT)<br>[$^{18}$F]-Fluoroethyltyrosine ([$^{18}$F]-FET)<br>[$^{11}$C]-Alpha-methyltryptophan<br>[$^{18}$F]-Proline |
| Amino acid transport and dopamine metabolism | [$^{18}$F]-Fluoro-L-3,4-dihydroxyphenylalanine ([$^{18}$F]-DOPA) |
| Cellular proliferation | 3-Deoxy-3-[$^{18}$F]-fluorothymidine ([$^{18}$F]-FLT)<br>[$^{18}$F]-2-Fluoro-5-methyl-1-beta-d-arabinofuranosyluracil ([$^{18}$F]-FMAU) |
| Lipid metabolism | $^{11}$C-Choline/<br>[$^{18}$F]-fluorocholine |
| Hypoxia | [$^{18}$F]-Fluoromisonidazole ([$^{18}$F]-FMISO)<br>[$^{123}$I]-Iodoazomycin arabinoside ([$^{123}$I]-IAZA)<br>[$^{18}$F]-Azomycin arabinoside ([$^{18}$F]-FAZA)<br>[$^{64}$Cu]-Methylthiosemicarbazone ([$^{64}$Cu]-ATSM) |
| Somatostatin receptor type 2 expression in meningiomas | [$^{68}$Ga]-DOTATOC<br>[$^{68}$Ga]-DOTATATE |

may occasionally be negligible. More interestingly, specificity of $^{11}$C-MET PET ranged between 87 and 100 % [35].

*Grading* On the other hand, the predictive value of $^{11}$C-MET PET for grading is limited. Several studies showed that $^{11}$C-MET is taken up by gliomas irrespective of grade and that there is sizeable overlap in uptake values between low-grade and high-grade gliomas. Semiquantitative analysis may help differentiating high-grade and low-grade gliomas in group analysis [35].

*Prognosis* In grades II and III gliomas, higher tumor to contralateral count ratios are associated with reduced survival. The prognostic power of $^{11}$C-MET was stronger than that of [$^{18}$F]-fluorodeoxyglucose ([$^{18}$F]-FDG) [34, 58] (Fig. 11.1).

*Tumor Extent Determination* The critical factor in determining the edges of the tumors is the method used for distinguishing significant from negligible tracer uptake. There is currently no consensus on the best method. Visual qualitative and several semiquantitative methods have been adopted: fixed percent threshold value of tumor uptake, tumor/non-tumor ratios, standardized uptake values (SUV), and automatic software-based segmentation algorithms are some examples of such techniques. Integrating [$^{11}$C]-MET PET with MR images is useful for planning surgery, with ensuing clinical impact in about 80 % of the procedures. Integration of $^{11}$C-MET PET with morphological imaging was also useful for defining the radiotherapy plan [45].

*Tumor Biopsy* Although the poor relation between $^{11}$C-MET uptake and grading does not allow predicting the highest tumor grade, $^{11}$C-MET PET may be used to reduce the number of required biopsy attempts and to reduce the risk of damaging functional areas in patients with brain tumors [45].

*Tumor Recurrence Versus Radiation Injury* Because of limitations of [$^{18}$F]-FDG for discriminating recurrent tumor from radiation injury,

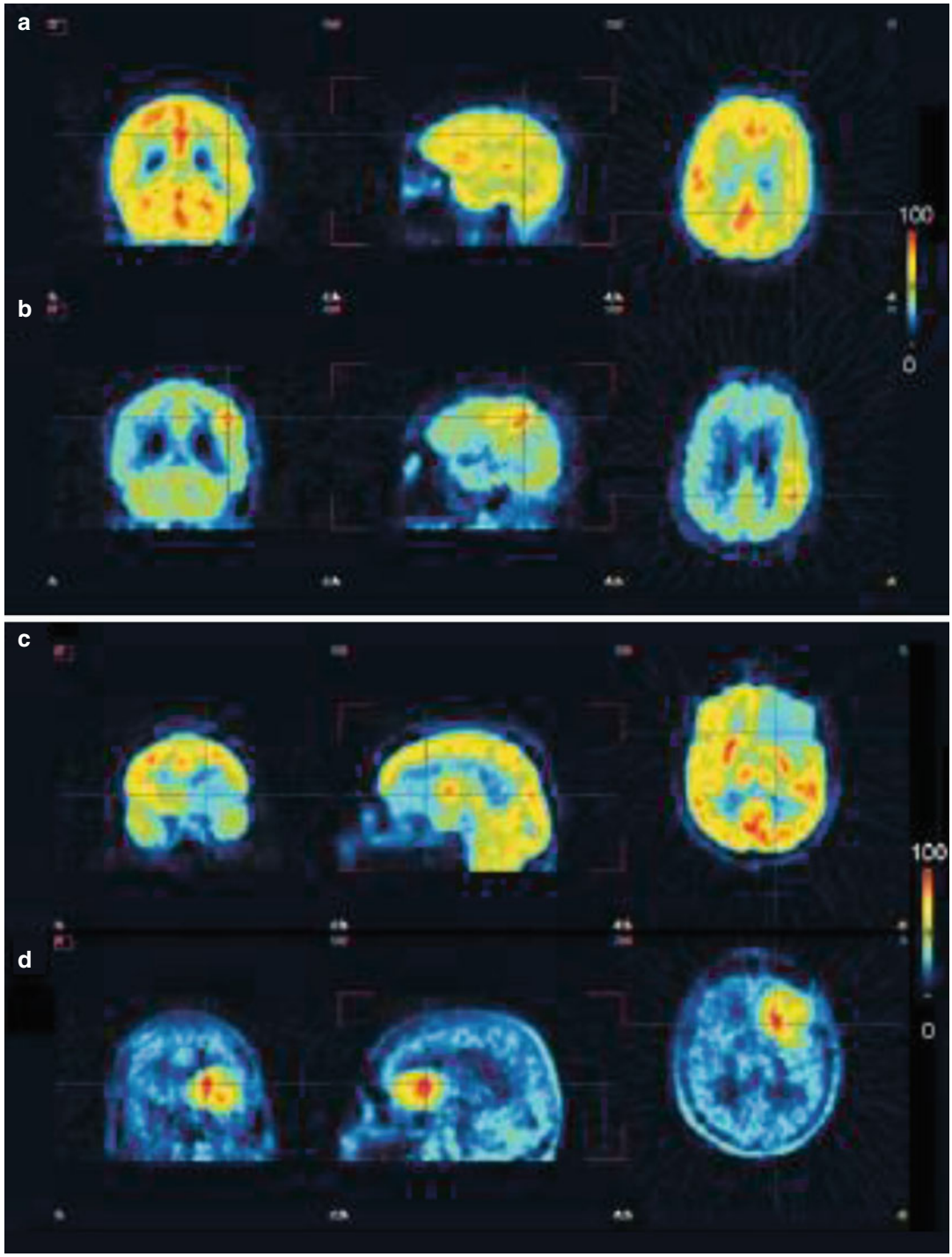


**Fig. 11.1** Combined [$^{18}$F]-FDG (*upper row*) and $^{11}$C-MET (*lower row*) PET studies. Patient #1 (**a**, **b**) displays tumor recurrence of the primary glioblastoma grade IV, which is easily detectable with $^{11}$C-MET (**b**) but not on [$^{18}$F]-FDG (**a**). Patient #2 (**c**, **d**) is affected by a primary oligoastrocytoma grade II, which is hot on $^{11}$C-MET PET (**d**) and cold on [$^{18}$F]-FDG PET (**c**) (Adapted from Van Laere et al. [58])

most authors prefer today using $^{11}$C-MET PET. Comparative evaluations show a greater accuracy of $^{11}$C-MET PET than [$^{18}$F]-FDG PET for the differential diagnosis [54].

### 11.2.2 O-(2-[$^{18}$F]-Fluoroethyl)-L-Tyrosine ([$^{18}$F]-FET) and 3-[$^{123}$I]-Alpha-Methyltyrosine ([$^{123}$I]-IMT)

[$^{18}$F]-FET is an artificial amino acid that is taken up into neoplastic cells, but it is not incorporated into proteins, in contrast to natural amino acids, such as $^{11}$C-MET, which has a 15 % incorporation rate [26, 61].

[$^{18}$F]-FET PET was shown to be more accurate than [$^{123}$I]-alpha-methyltyrosine, [$^{18}$F]-FDG, [$^{18}$F]-fluorothymidine, and [$^{18}$F]-fluorocholine to detect brain tumors.

A recent meta-analysis of published data of 13 studies on the use of [$^{18}$F]-FET PET in primary brain tumor including 462 patients showed sensitivity and specificity of 82 % and 76 %, respectively. The mean and maximum tumor-to-background ratio ($TBR_{mean}$ and $TBR_{max}$) were significantly lower in grade I–II gliomas as compared with III–IV gliomas [15].

The analysis of time–activity curves obtained through dynamic acquisition allows improving the differentiation between low- and high-grade gliomas. Early (<15 min) maximal uptake followed by a decreasing curve has been related to high-grade glioma, and late (>15 min) maximal uptake followed by a cumulative curve has been related to low-grade tumor [31].

[$^{18}$F]-FET imaging was also shown to have prognostic implications. In low-grade gliomas, baseline low [$^{18}$F]-FET uptake was predictive of longer time to progression and time to malignant transformation; on the contrary, high uptake predicted rapid conversion into a high-grade glioma [19]. [$^{18}$F]-FET can be used to quantify residual tumor volume after surgery, and postsurgical tumor volume determined by PET predicts progression-free and overall survival [44].

**Table 11.3** Factors affecting uptake of radiopharmaceuticals in gliomas

| |
|---|
| 1. Glucose metabolic rate |
| 2. Protein synthesis rate |
| 3. DNA proliferation rate |
| 4. Membrane (lipid) proliferation rate |
| 5. Blood–brain barrier integrity |
| 6. Histological grade |
| 7. Blood perfusion/blood volume |
| 8. Expression of membrane transporters |
| 9. Oxygen tissue concentration (hypoxia) |
| 10. Dimension of the lesion (partial volume effect) |
| 11. Radiotherapy treatment |
| 12. Treatment with steroids or oncologic drugs |
| 13. Necrotic areas |
| 14. Expression of catecholamine binding sites |

Some amino acid-derived radiopharmaceuticals (e.g., [$^{123}$I]-IMT) can also be labeled with single photon emitters for SPECT, allowing a less expensive, more widely accessible technique for imaging protein synthesis in brain tumors. As expected, worse tumor delineation was obtained in comparison to either $^{11}$C-MET or [$^{18}$F]-FET. However, high [$^{123}$I]-IMT uptake post-tumor resection is associated with shorter survival [60] (Table 11.3).

Among other amino acid tracers, a growing important role is being played by [$^{18}$F]-fluorodopa ([$^{18}$F]-FDOPA), which is also sensitive to dopamine metabolism. Other than the high physiological uptake in the striatum, this tracer also displays low uptake in all the remaining brain areas. [$^{18}$F]-DOPA PET/CT is highly sensitive and specific for detection of glioma recurrence, it is superior to [$^{18}$F]-FDG, and it is especially advantageous in patients with low-grade gliomas [32, 53] (Figs. 11.2 and 11.3).

**Tumor Proliferation** Increased cell proliferation rate is a well-known hallmark of cancer. 3-Deoxy-3-[$^{18}$F]-fluorothymidine ([$^{18}$F]-FLT) offers the advantages of [$^{18}$F]-labeling and a favorable radiometabolite profile. Kinetic analysis showed that patients with brain tumors have increased tracer incorporation ($K_i$). In high-grade tumors where blood flow is also increased, the

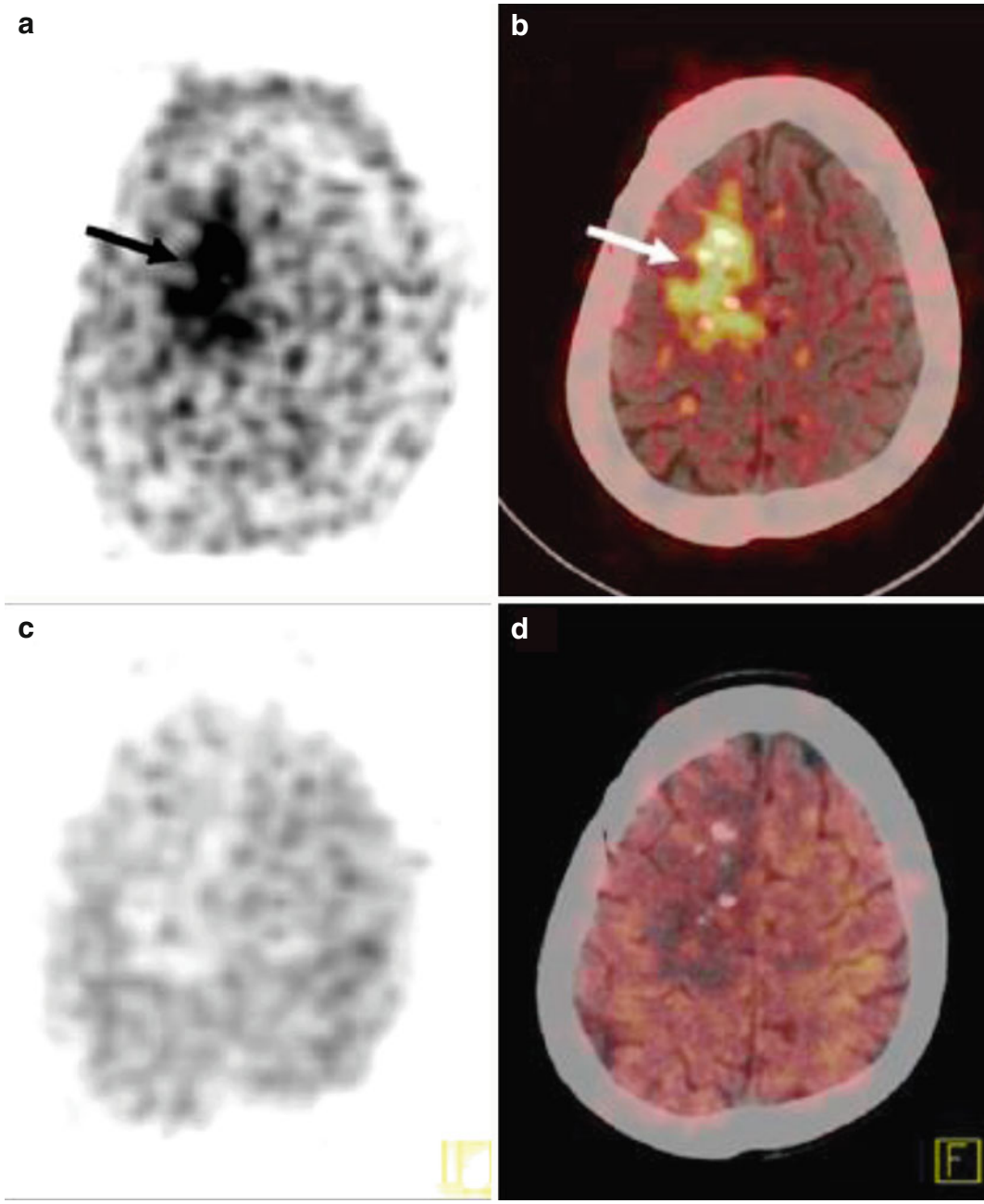


**Fig. 11.2** Combined [$^{18}$F]-DOPA (*upper row*) and [$^{18}$F]-FDG (*lower row*) PET studies. A 27-year-old man with right frontal grade II oligoastrocytoma treated primarily with surgery and radiotherapy, presented with clinical suspicion of recurrence. Transaxial [$^{18}$F]-DOPA PET (**a**) and PET/CT (**b**) images show tracer accumulation in the right frontal lobe lesion (*arrows*) suggestive of recurrence. Transaxial [$^{18}$F]-FDG PET (**c**) and PET/CT (**d**) images show no abnormal focus of tracer uptake and are negative for recurrence. The patient underwent reoperation and was found to have recurrent grade III glioma (anaplastic astrocytoma) on histopathology (Adapted from Karunanithi et al. [32])

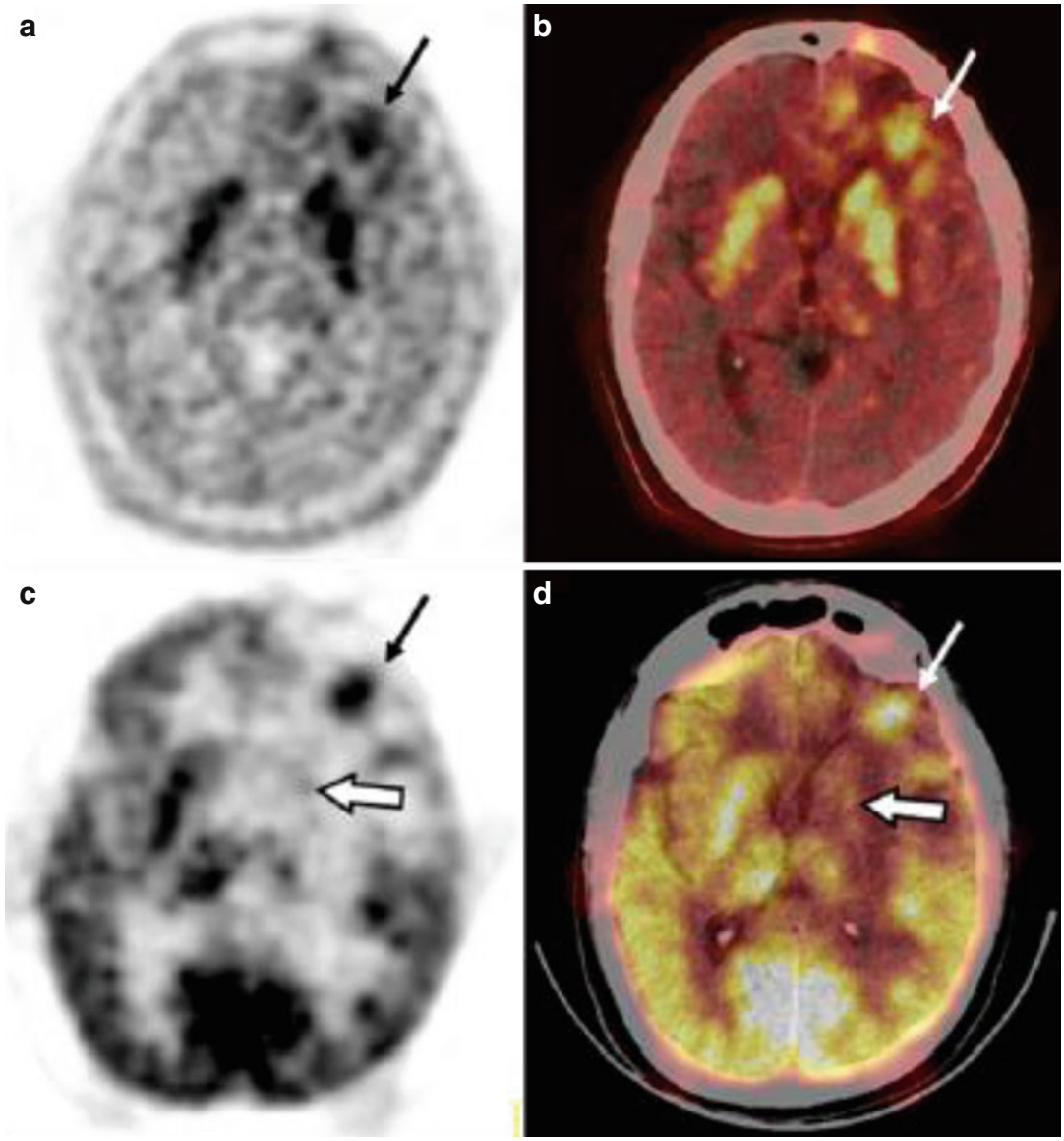


**Fig. 11.3** Combined [$^{18}$F]-DOPA (*upper row*) and [$^{18}$F]-FDG (*lower row*) PET studies. A 44-year-old man with left frontal grade IV glioblastomas multiforme treated primarily with surgery, radiotherapy, and temozolomide. He presented 18 months later with progressive severe headache. Transaxial [$^{18}$F]-FDOPA PET (**a**) and PET/CT (**b**) images show tracer accumulation in the left frontal lesion (*arrow*), suggestive of recurrence. Transaxial [$^{18}$F]-FDG PET (**c**) and PET/CT (**d**) images also show tracer accumulation in a left frontal lesion (*small arrows*), suggestive of recurrence. The patient died within 5 months of PET/CT with progressive neurological weakness. Both [$^{18}$F]-FDOPA PET/CT and [$^{18}$F]-FDG PET/CT were true positive for recurrence in this patient. Note the decrease in [$^{18}$F]-FDG uptake in the ipsilateral striatum (*large arrows*) due to postradiotherapy changes (Adapted from Karunanithi et al. [32])

increased tracer incorporation may partially be related to blood flow rather than metabolism [38] (Table 11.4).

[$^{18}$F]-FLT had slightly lower (83 %) sensitivity than $^{11}$C-MET (88 %) for detection of gliomas, and both tracers have a specificity of 100 %. $SUV_{max}$ for $^{11}$C-MET was significantly higher in high-grade gliomas than in low-grade gliomas, although there was a large overlap. For [$^{18}$F]-FLT, the group difference was larger. On the contrary, [$^{18}$F]-FLT was slightly superior to $^{11}$C-MET for tumor grading [24].

**Table 11.4** Most important favorable and unfavorable characteristics of common current radiopharmaceuticals for brain tumor imaging

| | Advantages | Disadvantages |
|---|---|---|
| [$^{18}$F]-FDG | Easily available, overall good accuracy, good quality images<br>Allows tumor grading<br>Correlates with prognosis | High physiological uptake in the normal brain<br>False positive by radiotherapy necrosis and infection<br>Limited role for definition of radiotherapy plan |
| Amino acid tracers | Available for PET and some limited availability for SPECT<br>Negligible uptake in the normal brain<br>Optimal tumor delineation and contrast<br>Uptake correlates with prognosis<br>Very high negative predictive value for distinguishing recurrence from necrosis<br>Useful for definition of radiotherapy plan | Tracer uptake is poorly affected by tumor grade<br>Uptake may be similar in low-grade gliomas and nonmalignant tumors |
| [$^{18}$F]-FLT | Negligible uptake in the normal brain<br>Optimal tumor delineation and contrast<br>Superior to amino acid tracers for grading<br>Allows differential diagnosis between tumor recurrence and necrosis | Uptake heavily affected by BBB integrity<br>Kinetic analysis with metabolite correction may be required |
| Other tracers (radiolabeled choline, hypoxia tracers, serotonin receptor tracers) | Capability to investigate other metabolic pathways of brain tumor metabolism | Presently, still experimental in the clinical setting |

### 11.2.3 [$^{18}$F]-Fluorodeoxyglucose ([$^{18}$F]-FDG)

PET with [$^{18}$F]-FDG allows measurement of the cerebral metabolic rate for glucose (CMRglc). [$^{18}$F]-FDG was the first PET tracer used for imaging brain tumors, and it is still widely used nowadays, after about 40 years. The 2-deoxyglucose model was defined by Sokoloff following autoradiographic experiments in rats [51]. Using arterial input function, dynamic scanning, and kinetic analysis, it is possible to obtain CMRglc (mg/100 g/min) [30, 51]. Using noninvasive approaches and a single static acquisition, SUV and the tumor/non-tumor ratio are the most commonly semiquantitative indices computed (Tables 11.5 and 11.6).

*Diagnosis and Grading* Early studies in brain tumor patients stressed the importance of the functional information provided by PET compared to morphologic neuroradiological techniques. Di Chiro et al. first used PET with [$^{18}$F]-FDG in 23 patients with cerebral gliomas. All ten high-grade gliomas demonstrated focal tracer uptake that was easily visible. The 13 low-grade gliomas had significantly lower CMRglc and no visible hot spot. In those early times, these results were considered as a major achievement because noninvasive grading of brain tumors was much less intuitive as nowadays. Sensitivity and specificity were 94 and 77 % [30] (Table 11.7).

Brain tumors may induce suppression of metabolic activity in the nearby normal and edematous tissue. Reduced glucose metabolism may occur also in the normal brain tissue remote, but functionally linked to the site of the tumor (crossed cerebellar diaschisis).

*Tumor Recurrence Versus Radiation Necrosis* Early studies showed that CMRglc was increased in patients with tumor recurrence and low in patients with necrosis [42]. Delayed imaging (90 min postinjection) increased the tumor-to-cortex contrast. Even though these results were confirmed in other studies, false positives were also reported because increased [$^{18}$F]-FDG accumulation may occur following radiotherapy.

The use of [$^{18}$F]-FDG for treatment planning remains controversial in light of the current

**Table 11.5** Characteristics of quantitative and semiquantitative brain PET studies with [$^{18}$F]-FDG

| | Quantitative studies | Qualitative studies |
|---|---|---|
| Arterial input function | Necessary | Not necessary |
| Acquisition | Dynamic (frames ranging from 30 s to 5 min for a total of 60 min) | Static (10–15 min acquisition 45-min postinjection) |
| Glycemia | Necessary | Not necessary |
| Parameters | CMRglc (mg/glc/100 g brain tissue) | Visual analysis<br>SUV<br>Tumor-to-non-tumor ratio |
| Data analysis | Time-consuming and technically challenging computer programming | None to simple (ROI analysis) |
| Diagnostic yield | Greater accuracy than semiquantitative analysis<br>Greater clinical impact not proven | Sufficient for the vast majority of clinical cases |
| Metabolic specificity | Not specific for tumor | Not specific for tumor |
| Advantages/pitfalls | Potentially very accurate/logistically demanding | Simple derivation/sensitive to many parameters |
| Application | Preferred for research studies and group analysis | Preferred for clinical diagnostic routine and single-subject evaluation |

**Table 11.6** Sensitivity and specificity for diagnosis of brain gliomas/gliomas recurrence for most common PET tracers[a]

| Tracer | Sensitivity (95 % CI) | Specificity (95 % CI) | Indication | Reference | Study |
|---|---|---|---|---|---|
| [$^{18}$F]-FDG | 94 % | 77 % | Diagnosis | [14] | Monocentric |
| [$^{18}$F]-FDG | 75 % | 81 % | Necrosis vs. recurrence | [11] | Monocentric |
| [$^{18}$F]-FDG | 0.77 (0.66–0.85) | 0.78 (0.54–0.91) | Necrosis vs. recurrence | [40] | Meta-analysis |
| [$^{11}$C]-MET | 0.70 (0.50–0.84) | 0.93 (0.44–1.0) | Necrosis vs. recurrence | [40] | Meta-analysis |
| [$^{11}$C]-MET | 75–95 % (range) | 87–100 % (range) | Diagnosis | [28] | Review |
| [$^{18}$F]-FET | 0.82 (0.74–0.88) | 0.76 (0.44–0.92) | Diagnosis | [15] | Meta-analysis |
| [$^{18}$F]-FLT | 79 % | 63 % | Diagnosis | [12] | Monocentric |

[a]Note that these values should be taken cautiously because they depend from several variables, including gold standard, clinical indication, tumor grade and dimension, sample size, analysis method, and type of study (single center, multicenter, or meta-analysis). Multitracer single studies are generally more informative for the comparison between two tracers. For these reasons, only some explicative studies are cited

widespread use of amino acid tracers. [$^{18}$F]-FDG might be of special interest in high-grade gliomas exhibiting marked intratumoral heterogeneity where hot spots could be possible targets for dose escalation.

**Prognostic Value and Response to Therapy**

Several studies indicate that glucose metabolism, at initial presentation, at recurrence, or in response to therapy, is predictive of survival. The semiquantitative evaluation in pretreatment [$^{18}$F]-FDG PET provides significant additional prognostic information in newly diagnosed high-grade tumors, it is statistically more robust than the visual evaluation, and it is independent of traditional prognostic factors. The mean survival time of patients exhibiting high CMRglu was shorter than in patients with low CMRglu [43]. In the subgroup of high-grade gliomas, it was possible to divide patients into a group with low and another with high metabolic activity with 1-year survival rates of 78 % and 29 %, respectively [3].

PET was useful for monitoring the response to chemotherapy. A recent publication based on the National Oncologic PET Registry examined retrospectively data from 479 patients with primary brain tumors (72 %) or brain metastasis (28 %)

**Table 11.7** Most common semiquantitative parameters, derivation, and main characteristics

| Parameter | Derivation | Advantages | Disadvantages |
|---|---|---|---|
| Standardized uptake value (SUV) | ROI placed on any brain region. The uptake is normalized to the injected dose and body mass weight | Automatically computed | Sensitive to many parameters, primarily successful tracer injection, interval from injection time, and scan time, glycemia, and variation in the input function |
| Tumor-to-background ratio (TBR) or tumor-to-normal cortex ratio (T/N) | Ratio between the tumor ROI and the contralateral (or other reference) normal brain region | Many global biases that affect the SUV are canceled out as the ratio is computed | Influenced by perfusion/blood volume effects |
| Tumor-to-white matter ratio | Ratio between the tumor ROI and a reference white matter region | See above | See above<br>Can only be applied to tumors that are strictly confined to gray matter |
| Parametric imaging | Kinetic analysis | Potentially very accurate | Very time consuming<br>Sensitive to biases of the input function<br>No clear advantage for the clinical routine. Used only in research protocols<br>Examples: CMRglc for [$^{18}$F]-FDG or $K_i$ for [$^{18}$F]-FLT |

and found that overall, [$^{18}$F]-FDG PET imaging changed the intended management in 38 % of patients [29].

**Radiolabeled Choline** Choline is a phospholipid precursor and participates to membrane proliferation. The radiolabeled tracer (either $^{11}$C-choline or [$^{18}$F]-fluorocholine) displayed an excellent capability to delineate the tumor contours due to the negligible uptake in the normal brain. However, increased tracer uptake may occur also in brain metastasis and meningiomas.

Presently there are discrepant findings on the issue whether increased lipid metabolism, as measured by PET/CT with radiolabeled, predicts [23, 41] or does not predict tumor grade [56]. Higher $^{11}$C-choline uptake has been reported in high-grade gliomas compared to low-grade gliomas [23]. This result was confirmed in a multitracer study; tracer uptake was significantly higher in high-grade gliomas than in low-grade gliomas for $^{11}$C-choline, but not for [$^{18}$F]-FDG [41]. However, $^{11}$C-choline PET/CT could not reliably differentiate between low-grade gliomas and benign lesions because of the low uptake in low-grade tumors [41]. Another multitracer study compared $^{11}$C-MET, $^{11}$C-choline, and [$^{18}$F]-FDG. Whereas all three tracers showed a similar correlation between the tumor-to-normal cortex ratio and tumor grade in astrocytic and oligodendroglial tumors, $^{11}$C-MET proved to best enable the straightforward visual localization of hot lesions [33].

**Imaging Tumor Hypoxia** Several bioreductive radiopharmaceuticals have been evaluated as hypoxia tracers. The common feature of these different tracers is that tissue binding increases as tissue oxygen decreases.

PET studies of brain tumor hypoxia are limited and focused mainly to the use of [$^{18}$F]-fluoromisonidazole ([$^{18}$F]-FMISO) [57]. Increased [$^{18}$F]-FMISO tumor uptake is generally found in the periphery but not in the necrotic center of glioblastomas multiforme. The latter finding is expected, because only peripheral viable cells are able to accumulate [$^{18}$F]-FMISO, and delivery to necrotic tissue is low [8].

Hypoxic volume measured with [$^{18}$F]-FMISO, that is, the voxels in the PET image with values higher than an arbitrary or predefined threshold, and the area of contrast enhancement in T1-weighted MR predict survival. [$^{18}$F]-FMISO uptake is greater in high-grade gliomas than in low-grade gliomas [52].

**Imaging Somatostatin Receptors in Meningiomas** Radiotracers able to visualize somatostatin receptors can be used for the delineation of meningiomas, based on the high expression of somatostatin receptor subtype 2 in these brain tumors [27]. The most commonly used tracer for this purpose is [$^{68}$Ga]-DOTATOC. PET imaging might detect lesions, with a higher sensitivity as compared with contrast-enhanced MRI, and help planning target volumes for radiation therapy, accurately distinguishing active meningioma tissue from surrounding postoperative tissue [1, 36]. The tracer has low intracranial background signal, given that somatostatin receptors are not expressed in the brain, except for the pituitary gland.

## 11.3 Additional Value of SPECT-CT and PET-CT Versus SPECT and PET Stand Alone

Radionuclide imaging has per se the capability of identifying disease in the early phase of disease, because biochemical dysfunctions typically occur before loss of structural function. Adding CT scan provides two major advantages: mainly it improved correction for attenuation of photons and secondarily it enables to locate on anatomical marks brain areas with abnormal functionality.

Low-dose CT is generally acquired with a tube current of 20–40 mA and tube voltage of about 120–140 kV; it is associated with low radiation doses of 1–4 mSv and is sufficient for anatomic referencing of SPECT lesions and attenuation correction [9]. The use of low-dose, nonenhanced spiral CT can be recommended in most SPECT/CT and PET/CT studies since virtually all patients referred to PET/CT or SPECT/CT will have already performed a diagnostic CT or MR. In the opposite case, diagnostic CT with contrast media should be performed [9].

So far, data on the added value of hybrid PET/CT and SPECT/CT over the stand-alone PET and SPECT remain rather limited. In general, individual CT scan-based attenuation correction may be particularly important for tracers with important regional variations in binding (such as [$^{18}$F]-FDOPA), but the same could apply to tracers that display more homogenous distribution, such as [$^{18}$F]-FDG or many amino acid tracers. It has been shown that attenuation correction based on individual CT scans produces more accurate results than attenuation correction based on ellipse-based Chang method [25].

One study showed that SPECT/CT could be useful to locate tumors in the presurgical setting and that this information could be transferred to the definition of the radiotherapy plan and for monitoring therapy. SPECT/CT technique allows to distinguish brain tumors and from other brain region with physiological uptake of the radiotracer, such as choroid plexus and venous sinuses, with a proven clinical impact on management in 43 % of patients [16].

## 11.4 PET/MRI: The New Modality of Choice for Brain Tumor Imaging?

PET/MRI tomographs represent the latest development in hybrid molecular imaging, opening new perspectives for clinical and research applications and attracting a large interest within the medical community [48, 59]. This new hybrid modality is expected to play a relevant role in a number of clinical applications in oncology, cardiology, and neuroimaging. Indeed, for brain imaging, MRI is the

"morphological" modality of choice for the investigation of brain lesions and clearly outperforms the non-contrast-enhanced CT which is usually coupled to PET studies in the current hybrid PET/CT examinations [18]. MRI provides not only an excellent soft tissue contrast, enhanced by the use of gadolinium-based contrast agents, but also visualizes white matter tracts, by diffusion tensor imaging (DTI), of utmost importance in surgical planning. In addition, a number of functional parameters can also be obtained by MRI, namely, perfusion, diffusion, and metabolic changes using MR spectroscopy.

### 11.4.1 PET/MRI Integrated Systems

Even if the idea of hybrid PET/MRI imaging is not new, and the first prototypes for small animal imaging date back to the early 1990s, the first hybrid acquisition in humans in a dedicated brain system has been realized in 2008 [49]. This is due to the major challenges arising when bringing these two technologies together, namely, the intrinsic incompatibility of photomultiplier technology with the magnetic field.

Different solutions have been adopted and can be grouped in two categories:

1. Simultaneous systems in which the PET is within the magnetic field and replacing the PET detection system, classically based on photomultipliers, by magnetic field-insensitive avalanche photodiodes or silicon-based elements [13, 47]
2. Sequential systems, in which each component (MRI and PET) is almost identical to standard standalone systems, provided proper electromagnetic shielding [62]

While the first solution has the clear advantage of simultaneous acquisition of both PET and MRI, with an overall reduction of total examination time, the second solution could be adopted without changes in the PET technology and allowed time-of-flight (TOF) imaging since the beginning. One of the two simultaneous tomographs currently available now also provides TOF technology [47].

### 11.4.2 PET/MRI Studies in Brain Oncology

Only a few studies have so far investigated the information provided by hybrid PET/MRI for brain tumor assessment and they are recapitulated in Table 11.8.

They overall show the feasibility of intracranial mass characterization by integrated PET/MRI also for presurgical and radiation therapy planning and also in pediatric patients (two studies targeted specifically this population). The majority of studies included patients with glioma and a subpopulation of patients with meningiomas, using a variety of PET tracers. The studies comparing PET/MRI output with PET/CT overall show that, despite systematic quantitative differences with PET/CT, mainly due to the attenuation correction strategy adopted, the image contrast and visual interpretation of the images obtained with PET/MRI are comparable to PET/CT.

The added value of integrated PET/MRI tomograph compared with the current standard (fused PET and MRI images acquired in separate sessions) has not been specifically investigated yet, and no cost-effectiveness studies are available yet.

Finally, most of these studies adopted fully diagnostic protocols of each modality, resulting in lengthy acquisitions. A key issue, to be addressed in future studies and with a wider practice with integrated tomographs, will be the identification of complementary/redundant information provided by PET and MRI, in order to develop truly integrated protocols that take advantage of the strongest assets of each modality, avoiding the duplication of data [4].

Hybrid PET/MRI systems are also the ideal setting for answering specific research questions,

**Table 11.8** PET/MRI studies in brain tumors

| Study | N of patients evaluated for intracranial lesions | Clinical indications | Type of PET-MR tomograph | Radiotracers | Results |
|---|---|---|---|---|---|
| Boss et al. [7] | 4 adult patients | Staging | Simultaneous (whole-body 3 T MR with BrainPET insert, Siemens Healthcare) | [$^{11}$C]-MET | Comparison of DTI acquired simultaneously to PET or after the removal of the PET insert: the presence of the insert induces some artifacts but does not hinder diagnostic interpretation of DTI images |
| Boss et al. [6] | 10 adult patients | Staging | Simultaneous (whole-body 3 T MR with BrainPET insert, Siemens Healthcare) | [$^{11}$C]-MET [$^{68}$Ga]-DOTATOC | Comparison with PET/CT data: PET/MRI data were strictly comparable, also for quantitative aspects and calculated tumor volumes |
| Schwenzer et al. [50] | 28 adult patients | Staging and restaging | Simultaneous (whole-body 3 T MR with BrainPET insert, Siemens Healthcare) | [$^{18}$F]-FDG [$^{11}$C]-MET [$^{68}$Ga]-DOTATOC | Comparison of PET/MRI and PET/CT data: comparable tumor delineation with [$^{11}$C]-methionine; additional lesions were found in [$^{68}$Ga]-DOTATOC-PET images obtained with PET/MRI (presumably related to the higher resolution of the PET insert) |
| Neuner et al. [39] | 4 adult patients | Staging and restaging of gliomas | Simultaneous (whole-body 3 T MR with BrainPET insert, Siemens Healthcare) | [$^{18}$F]-FET | Description of acquisition protocols, obtaining diagnostic quality and comprehensive evaluation of gliomas in one examination |
| Thorwarth et al. [55] | 3 adult patients | Restaging and radiation therapy planning of atypical meningiomas | Simultaneous (whole-body 3 T MR with BrainPET insert, Siemens Healthcare) | [$^{68}$Ga]-DOTATOC | Description of adapted acquisition protocols and discussion of potential logistic and diagnostic benefits of integrated PET/MRI in radiation therapy planning of meningiomas |
| Garibotto et al. [22] | 5 adult patients | Staging and radiotherapy planning | Sequential (Philips Ingenuity TF) | [$^{18}$F]-FET | Description of adapted acquisition protocols, obtaining diagnostic quality and comprehensive evaluation of gliomas in one examination |

**Table 11.8** (continued)

| Study | N of patients evaluated for intracranial lesions | Clinical indications | Type of PET-MR tomograph | Radiotracers | Results |
|---|---|---|---|---|---|
| Bisdas et al. [5] | 28 adult patients | Biopsy planning in gliomas | Simultaneous (Siemens mMR) | [$^{11}$C]-MET | Comparison of the areas of the metabolic imaging provided by [$^{11}$C]-MET PET and magnetic resonance spectroscopy: the maps overlap only partially with different results depending on tumor grade |
| Filss et al. [17] | 36 adult patients | Staging and restaging | Simultaneous (whole-body 3 T MR with BrainPET insert, Siemens Healthcare) | [$^{18}$F]-FET | Comparison of [$^{18}$F]-FET uptake and perfusion-weighted MRI: significant differences in the spatial localization and size of metabolically active and hyperperfused tissue in gliomas |
| Preuss et al. [46] | 4 pediatric patients | Biopsy planning | Simultaneous (Siemens mMR) | [$^{11}$C]-MET | Description of adapted acquisition protocols, obtaining all necessary data for surgical planning and neuronavigation in one single session |
| Fraioli et al. [20] | 12 pediatric patients | Staging and restaging of astrocytic tumors | Simultaneous (whole-body 3 T MR with BrainPET insert, Siemens Healthcare) | [$^{18}$F]-Fluorocholine | Description of adapted acquisition protocols and discussion of potential logistic and diagnostic benefits of integrated PET/MRI in astrocytic brain tumors in children |
| Afshar-Oromieh et al. [2] | 15 adult patients | Detection and radiation therapy volume definition of meningiomas | Simultaneous (Siemens mMR) | [$^{68}$Ga]-DOTATOC | Comparison of PET/CT and PET/MR: ideal diagnostic quality and lesion definition on PET/MRI images, despite systematic differences in quantitative parameters, possibly due to the later acquisition of PET/MRI images and to the different PET detectors |

namely, about the similarity between functional measures obtained by PET and MRI. One study has specifically investigated areas of regional cerebral blood volume, estimated on perfusion-weighted MRI, and increased amino acidic uptake evaluated by [$^{18}$F]-FET PET, showing that the overlap between the two processes is limited in gliomas [17]. Another study evaluated the overlap between changes in MR spectroscopy and 11C-MET uptake, showing a partial overlap and different in low- and high-grade gliomas [5]. Overall, these preliminary studies underline the diversity of the information provided by the two modalities and the need for further cross-validation studies.

Advantages and challenges associated with this new hybrid modality, specifically concerning neuroimaging applications, have been previously addressed [10, 21].

We only briefly summarize here the main advantages of PET/MR hybrid imaging, as compared with standard PET/CT, which we could observe in our clinical practice:

- The availability of all relevant information in a single session, which reduces total examination time. The patient only has to be positioned once: this issue is particularly important for patients with limited compliance, such as children or patients with cognitive impairment due to neurodegenerative disorders or brain lesions. The single imaging session is also an advantage when additional procedures, such as anesthesia or sedation, are required. In general, patients and caregivers appreciate the opportunity of gathering all data in a single session.
  The acquisition at the same time of all image series also guarantees that all variables related to the disease evolution and to the treatment effects are strictly identical for all modalities, while PET and MRI acquired separately might easily have an interval of some days, with the possibility of relevant changes in some rapidly evolving biological phenomena
- A lower radiation exposure, by avoiding the CT acquisition currently used in PET/CT scans for attenuation measurement. This gain is of special interest in the pediatric population and in cases requiring repeated investigations.
- The systematic integration of PET and MRI for image interpretation. Fusion of images acquired on separate systems is standard practice and has already proven its importance and the diagnostic gain associated [37]. This can be ideally achieved by a combined hybrid acquisition, which minimizes fusion issues. In addition, the acquisition of all images in single session encourages truly multidisciplinary reading of the PET and MRI dataset, with an added value coming from the joined interpretation of the findings of the two modalities.

## Conclusions

PET/CT can be used nowadays with several radiopharmaceuticals for imaging gliomas. At initial staging PEt allows identification of the metabolically active tumor volume, which is essential information to direct biopsy, for planning surgery and radiotherapy and can clarify an undetermined finding on MRI. PET can be used to assess noninvasively tumor grading: high metabolic activity is predictive of higher tumor grade and proliferative activity and it has negative prognostic value. Hardware-based coregistration of PET to CT is standard today, and it helps the differential diagnosis between tumor recurrence and radiation injury. When feasible, hardware- or software-based registration to MRI should also be performed. Increased PET activity combined with increased contrast enhancement or T1/T2 abnormalities is consistent with tumor recurrence; negligible PET activity is consistent with radiation necrosis.

[$^{18}$F]-FDG has high physiological brain uptake in gray matter und suffers from specificity, so that radiation necrosis can occasionally be indistinguishable from recurrent high-grade tumor. However, tumor [$^{18}$F]-FDG uptake has prognostic value.

Several radiopharmaceuticals were subsequently developed to explore biochemical processes other than glucose metabolism

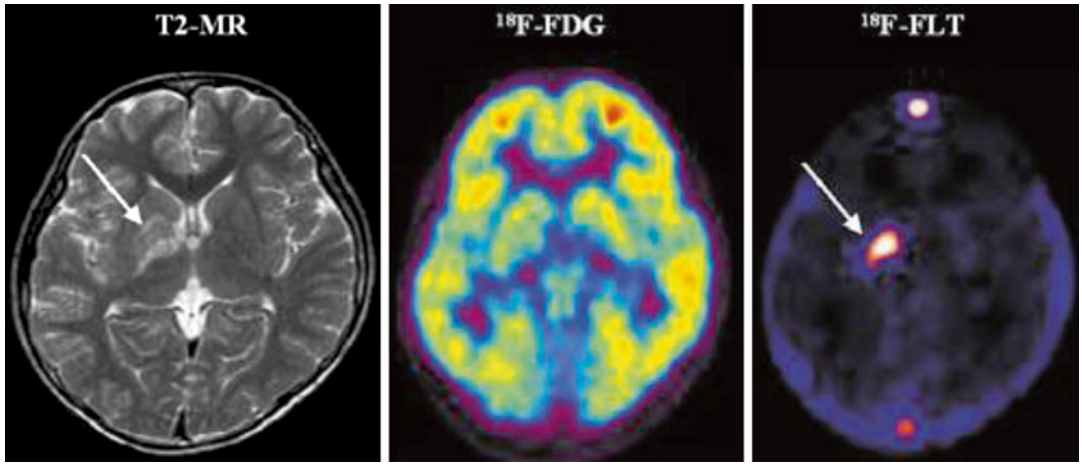


**Fig. 11.4** An 11-year-old male with a germ cell tumor of the basal ganglia. MR shows subtle changes (*arrow*) in the right basal ganglia. On [$^{18}$F]-FDG PET, the right basal ganglia lesion shows slightly decreased uptake compared with the contralateral basal ganglia but increased uptake compared with normal *white matter*. [$^{18}$F]-FLT PET, however, reveals intensely increased uptake, suggesting the presence of a malignant tumor (*arrow*). Based on the [$^{18}$F]-FLT PET results, a stereotactic biopsy could be performed in the right basal ganglia (Adapted from Choi et al. [12])

that are associated to tumor growth. Amino acid tracers are sensitive to transport across the BBB and, to some extent, protein synthesis. Among these tracers, $^{11}$C-MET is the one that is more widely used. Other promising tracers include [$^{18}$F]-FET and [$^{18}$F]-DOPA. For [$^{18}$F]-FET, a SPECT analog ([$^{123}$I]-IMT) exists that has lower diagnostic but similar prognostic values. Other than that, the role of SPECT/CT has today dramatically decreased. Physiological brain uptake of amino acids is low and they are less involved in inflammation in respect to [$^{18}$F]-FDG. Thus, their specificity for differentiating tumor recurrence vs. radiation necrosis is higher. However, amino acid tracers may be taken up similarly by low-grade tumors and high-grade tumors so that grading is not accurately predicted. They also have limited accuracy to distinguish low-grade gliomas from nonmalignant lesions. Virtually all amino acid tracers can be used for presurgical evaluation and to predict survival. For the clinical routine, the role of other tracers, such as hypoxia tracers and radiolabeled choline, is more uncertain (Fig. 11.4).

An ongoing technological development that may substantially increase the diagnostic accuracy of current PET tomographs and reduce logistical difficulties is the further development of PET/MRI tomographs. The studies performed so far have consistently shown that PET/MRI tomographs provide all relevant information for disease staging, biopsy, surgery, or radiation therapy planning in a single session, with adequate diagnostic quality despite the technical complexity of the hybrid design. As compared with PET/CT and MRI acquired separately, the hybrid design has mainly logistic and practical advantages: one single imaging session and identical conditions for both modalities. The diagnostic gain is still to be proven, even if the availability of high-resolution morphological imaging and functional/molecular imaging at the same time is expected to increase diagnostic confidence and possibly decrease false-positive and false-negative findings derived from each modality alone. Brain tumor imaging will clearly be one of the indications of choice for the new PET/MRI hybrid tomographs, where available (Fig. 11.5).

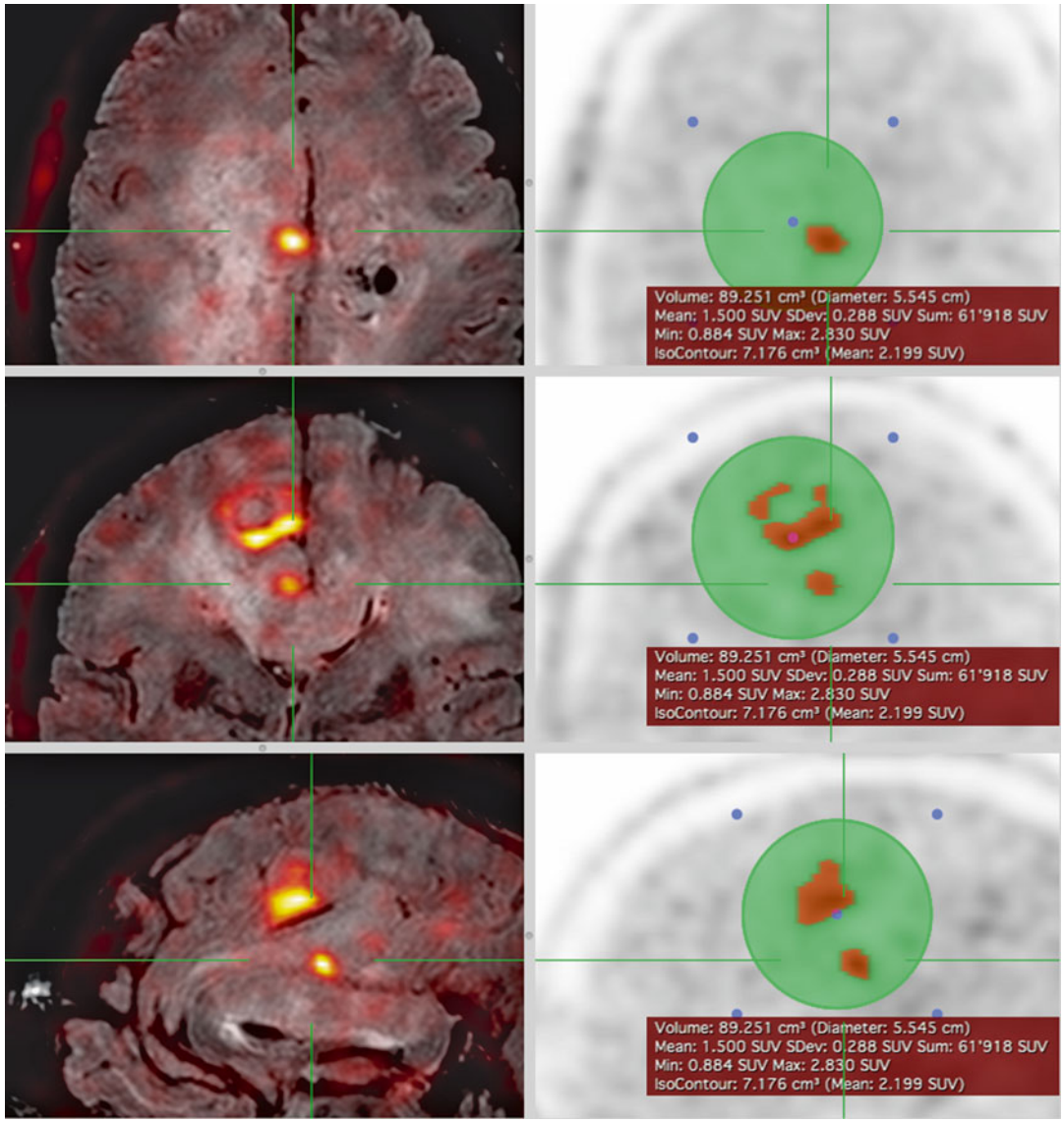


**Fig. 11.5** PET/MRI images of [$^{18}$F]-FET in a 53-year-old glioblastoma patient, showing the fusion of FLAIR MRI and PET images (*left panel*) and the segmentation of the areas with the higher uptake (threshold set at 70% of the $SUV_{max}$) (*right panel*) (Geneva University Hospitals, Geneva, Switzerland)

## References

1. Afshar-Oromieh A, Giesel FL et al (2012) Detection of cranial meningiomas: comparison of (6)(8) Ga-DOTATOC PET/CT and contrast-enhanced MRI. Eur J Nucl Med Mol Imaging 39(9):1409–1415
2. Afshar-Oromieh A, Wolf MB et al (2015) Comparison of (6)(8)Ga-DOTATOC-PET/CT and PET/MRI hybrid systems in patients with cranial meningioma: initial results. Neuro Oncol 17(2):312–319
3. Alavi JB, Alavi A et al (1988) Positron emission tomography in patients with glioma. A predictor of prognosis. Cancer 62(6):1074–1078
4. Barbosa Fde G, von Schulthess G et al (2015) Workflow in simultaneous PET/MRI. Semin Nucl Med 45(4):332–344
5. Bisdas S, Ritz R et al (2013) Metabolic mapping of gliomas using hybrid MR-PET imaging: feasibility of the method and spatial distribution of metabolic changes. Invest Radiol 48(5):295–301

6. Boss A, Bisdas S et al (2010) Hybrid PET/MRI of intracranial masses: initial experiences and comparison to PET/CT. J Nucl Med 51(8):1198–1205
7. Boss A, Kolb A et al (2010) Diffusion tensor imaging in a human PET/MR hybrid system. Invest Radiol 45(5):270–274
8. Bruehlmeier M, Roelcke U et al (2004) Assessment of hypoxia and perfusion in human brain tumors using PET with 18F-fluoromisonidazole and 15O-H2O. J Nucl Med 45(11):1851–1859
9. Buck AK, Nekolla S et al (2008) Spect/Ct. J Nucl Med 49(8):1305–1319
10. Catana C, Drzezga A et al (2012) PET/MRI for neurologic applications. J Nucl Med 53(12):1916–1925
11. Chao ST, Suh JH et al (2001) The sensitivity and specificity of FDG PET in distinguishing recurrent brain tumor from radionecrosis in patients treated with stereotactic radiosurgery. Int J Cancer 96(3):191–197
12. Choi SJ, Kim JS et al (2005) [18F]3'-deoxy-3'-fluorothymidine PET for the diagnosis and grading of brain tumors. Eur J Nucl Med Mol Imaging 32(6):653–659
13. Delso G, Furst S et al (2011) Performance measurements of the Siemens mMR integrated whole-body PET/MR scanner. J Nucl Med 52(12):1914–1922
14. Di Chiro G, DeLaPaz RL et al (1982) Glucose utilization of cerebral gliomas measured by [18F] fluorodeoxyglucose and positron emission tomography. Neurology 32(12):1323–1329
15. Dunet V, Rossier C et al (2012) Performance of 18F-fluoro-ethyl-tyrosine (18F-FET) PET for the differential diagnosis of primary brain tumor: a systematic review and Metaanalysis. J Nucl Med 53(2):207–214
16. Filippi L, Schillaci O et al (2006) Usefulness of SPECT/CT with a hybrid camera for the functional anatomical mapping of primary brain tumors by [Tc99m] tetrofosmin. Cancer Biother Radiopharm 21(1):41–48
17. Filss CP, Galldiks N et al (2014) Comparison of 18F-FET PET and perfusion-weighted MR imaging: a PET/MR imaging hybrid study in patients with brain tumors. J Nucl Med 55(4):540–545
18. Fink J, Muzi M et al (2015) Multi-modality brain tumor imaging – MRI, PET, and PET/MRI. J Nucl Med 56(10):1554–1561
19. Floeth FW, Pauleit D et al (2007) Prognostic value of O-(2-18F-fluoroethyl)-L-tyrosine PET and MRI in low-grade glioma. J Nucl Med 48(4):519–527
20. Fraioli F, Shankar A et al (2015) 18F-fluoroethylcholine (18F-Cho) PET/MRI functional parameters in pediatric astrocytic brain tumors. Clin Nucl Med 40(1):e40–e45
21. Garibotto V, Forster S et al (2013) Molecular neuroimaging with PET/MRI. Clin Transl Imaging 1(1):53–63
22. Garibotto V, Heinzer S et al (2013) Clinical applications of hybrid PET/MRI in neuroimaging. Clin Nucl Med 38(1):e13–e18
23. Hara T, Kondo T et al (2003) Use of 18F-choline and 11C-choline as contrast agents in positron emission tomography imaging-guided stereotactic biopsy sampling of gliomas. J Neurosurg 99(3):474–479
24. Hatakeyama T, Kawai N et al (2008) 11C-methionine (MET) and 18F-fluorothymidine (FLT) PET in patients with newly diagnosed glioma. Eur J Nucl Med Mol Imaging 35(11):2009–2017
25. Hayashi M, Deguchi J et al (2005) Comparison of methods of attenuation and scatter correction in brain perfusion SPECT. J Nucl Med Technol 33(4):224–229
26. Heiss P, Mayer S et al (1999) Investigation of transport mechanism and uptake kinetics of O-(2-[18F] fluoroethyl)-L-tyrosine in vitro and in vivo. J Nucl Med 40(8):1367–1373
27. Henze M, Schuhmacher J et al (2001) PET imaging of somatostatin receptors using [68GA]DOTA-D-Phe1-Tyr3-octreotide: first results in patients with meningiomas. J Nucl Med 42(7):1053–1056
28. Herholz K, Langen KJ et al (2012) Brain tumors. Semin Nucl Med 42(6):356–370
29. Hillner BE, Siegel BA et al (2011) Impact of dedicated brain PET on intended patient management in participants of the national oncologic PET Registry. Mol Imaging Biol 13(1):161–165
30. Huang SC, Phelps ME et al (1981) Error sensitivity of fluorodeoxyglucose method for measurement of cerebral metabolic rate of glucose. J Cereb Blood Flow Metab 1(4):391–401
31. Jansen NL, Graute V et al (2012) MRI-suspected low-grade glioma: is there a need to perform dynamic FET PET? Eur J Nucl Med Mol Imaging 39(6): 1021–1029
32. Karunanithi S, Sharma P et al (2013) 18F-FDOPA PET/CT for detection of recurrence in patients with glioma: prospective comparison with 18F-FDG PET/CT. Eur J Nucl Med Mol Imaging 40(7):1025–1035
33. Kato T, Shinoda J et al (2008) Metabolic assessment of gliomas using 11C-methionine, [18F] fluorodeoxyglucose, and 11C-choline positron-emission tomography. AJNR Am J Neuroradiol 29(6):1176–1182
34. Kim S, Chung JK et al (2005) 11C-methionine PET as a prognostic marker in patients with glioma: comparison with 18F-FDG PET. Eur J Nucl Med Mol Imaging 32(1):52–59
35. Kubota R, Kubota K et al (1995) Methionine uptake by tumor tissue: a microautoradiographic comparison with FDG. J Nucl Med 36(3):484–492
36. Milker-Zabel S, Zabel-du Bois A et al (2006) Improved target volume definition for fractionated stereotactic radiotherapy in patients with intracranial meningiomas by correlation of CT, MRI, and [68Ga]-DOTATOC-PET. Int J Radiat Oncol Biol Phys 65(1):222–227
37. Morana G, Piccardo A et al (2014) Value of 18F-3,4-dihydroxyphenylalanine PET/MR image fusion in pediatric supratentorial infiltrative astrocytomas: a prospective pilot study. J Nucl Med 55(5):718–723
38. Muzi M, Spence AM et al (2006) Kinetic analysis of 3'-deoxy-3'-18F-fluorothymidine in patients with gliomas. J Nucl Med 47(10):1612–1621
39. Neuner I, Kaffanke JB et al (2012) Multimodal imaging utilising integrated MR-PET for human brain tumour assessment. Eur Radiol 22(12):2568–2580

40. Nihashi T, Dahabreh IJ et al (2013) Diagnostic accuracy of PET for recurrent glioma diagnosis: a meta-analysis. AJNR Am J Neuroradiol 34(5):944–950, S941-911
41. Ohtani T, Kurihara H et al (2001) Brain tumour imaging with carbon-11 choline: comparison with FDG PET and gadolinium-enhanced MR imaging. Eur J Nucl Med 28(11):1664–1670
42. Patronas NJ, Di Chiro G et al (1982) Work in progress: [18F] fluorodeoxyglucose and positron emission tomography in the evaluation of radiation necrosis of the brain. Radiology 144(4):885–889
43. Patronas NJ, Di Chiro G et al (1985) Prediction of survival in glioma patients by means of positron emission tomography. J Neurosurg 62(6):816–822
44. Piroth MD, Holy R et al (2011) Prognostic impact of postoperative, pre-irradiation (18)F-fluoroethyl-l-tyrosine uptake in glioblastoma patients treated with radiochemotherapy. Radiother Oncol 99(2):218–224
45. Pirotte BJ, Levivier M et al (2009) Positron emission tomography-guided volumetric resection of supratentorial high-grade gliomas: a survival analysis in 66 consecutive patients. Neurosurgery 64(3):471–481
46. Preuss M, Werner P et al (2014) Integrated PET/MRI for planning navigated biopsies in pediatric brain tumors. Childs Nerv Syst 30(8):1399–1403
47. Queiroz MA, Delso G et al (2015) Dose optimization in TOF-PET/MR compared to TOF-PET/CT. PLoS One 10(7):e0128842
48. Ratib O, Beyer T (2011) Whole-body hybrid PET/MRI: ready for clinical use? Eur J Nucl Med Mol Imaging 38(6):992–995
49. Schlemmer HP, Pichler BJ et al (2008) Simultaneous MR/PET imaging of the human brain: feasibility study. Radiology 248(3):1028–1035
50. Schwenzer NF, Stegger L et al (2012) Simultaneous PET/MR imaging in a human brain PET/MR system in 50 patients-current state of image quality. Eur J Radiol 81(11):3472–3478
51. Sokoloff L, Reivich M et al (1977) The [14C]deoxyglucose method for the measurement of local cerebral glucose utilization: theory, procedure, and normal values in the conscious and anesthetized albino rat. J Neurochem 28(5):897–916
52. Swanson KR, Chakraborty G et al (2009) Complementary but distinct roles for MRI and 18F-fluoromisonidazole PET in the assessment of human glioblastomas. J Nucl Med 50(1):36–44
53. Talbot JN, Kerrou K et al (2007) FDOPA PET has clinical utility in brain tumour imaging: a proposal for a revision of the recent EANM guidelines. Eur J Nucl Med Mol Imaging 34(7):1131–1132, author reply 1133–1134
54. Terakawa Y, Tsuyuguchi N et al (2008) Diagnostic accuracy of 11C-methionine PET for differentiation of recurrent brain tumors from radiation necrosis after radiotherapy. J Nucl Med 49(5):694–699
55. Thorwarth D, Muller AC et al (2013) Combined PET/MR imaging using (68)Ga-DOTATOC for radiotherapy treatment planning in meningioma patients. Recent Results Cancer Res 194:425–439
56. Utriainen M, Komu M et al (2003) Evaluation of brain tumor metabolism with [11C]choline PET and 1H-MRS. J Neurooncol 62(3):329–338
57. Valk PE, Mathis CA et al (1992) Hypoxia in human gliomas: demonstration by PET with fluorine-18-fluoromisonidazole. J Nucl Med 33(12):2133–2137
58. Van Laere K, Ceyssens S et al (2005) Direct comparison of 18F-FDG and 11C-methionine PET in suspected recurrence of glioma: sensitivity, inter-observer variability and prognostic value. Eur J Nucl Med Mol Imaging 32(1):39–51
59. von Schulthess GK, Veit-Haibach P (2015) Guest editorial. Semin Nucl Med 45(3):189–191
60. Weber W, Bartenstein P et al (1997) Fluorine-18-FDG PET and iodine-123-IMT SPECT in the evaluation of brain tumors. J Nucl Med 38(5):802–808
61. Wester HJ, Herz M et al (1999) Synthesis and radiopharmacology of O-(2-[18F]fluoroethyl)-L-tyrosine for tumor imaging. J Nucl Med 40(1):205–212
62. Zaidi H, Ojha N et al (2011) Design and performance evaluation of a whole-body Ingenuity TF PET-MRI system. Phys Med Biol 56(10):3091–3106